Framework Materials

DOI: 10.1002/anie.201001675

Porous Metal Carboxylate Boron Imidazolate Frameworks**

Shoutian Zheng, Tao Wu, Jian Zhang, Mina Chow, Ruben A. Nieto, Pingyun Feng, and Xianhui Bu**

Metal–organic frameworks (MOFs) have attracted considerable interest because of their intriguing structures and potential applications.[1] Of particular importance is the design and synthesis of MOFs with novel composition and topology, because properties and applications of such materials depend on their composition and topology. Among MOFs, metal–carboxylate frameworks (MCFs) constitute one of the most important subclasses and have been studied extensively.[2–6] Some well-known porous MCFs include HKUST-1,[3a] MOF-5,[3b] and MIL-101.[3c] In addition to MCFs, porous frameworks constructed from heterocyclic ligands (e.g., zeolitic imidazolate frameworks, ZIFs) and di- and trivalent cations such as Zn^{2+} and In^{3+}[7,8] have also been developed. More recently, boron imidazolate frameworks (BIFs) based on boron imidazolate complexes were reported.[9] Ultralightweight elements such as B and Li (e.g., in BIF-9 with the zeolite RHO net), together with the strong covalent bond (B–N), hold promise for the development of stable low-density porous solids with potential applications such as on-board gas-storage materials.

In MCFs, ZIFs, and BIFs, the cross-linking ligands (carboxylates, imidazolates, and boron imidazolates, respectively) have different properties, leading to porous frameworks with distinct structural features and properties. Herein, we are interested in unifying these different structural modes in the same framework to create a family of materials called metal carboxylate boron imidazolate frameworks (MC-BIFs). Such a multicomponent system can lead to greater compositional and topological diversity. As a first step, divalent metal ions widely used for MCFs and ZIFs were chosen for this work, because M^{2+} ions have a strong affinity for both carboxylates and imidazolates, making it possible to combine carboxylate and $[B(im)_4]^-$ in the same framework without phase separation (im = imidazolate).

[*] Dr. S. Zheng, Dr. J. Zhang, M. Chow, R. A. Nieto, Prof. Dr. X. Bu
Department of Chemistry and Biochemistry
California State University, Long Beach
1250 Bellflower Boulevard, Long Beach, CA 90840 (USA)
Fax: (+1) 562-985-8557
E-mail: xbu@csulb.edu
T. Wu, Prof. Dr. P. Feng
Department of Chemistry, University of California
Riverside, CA 92521 (USA)
E-mail: pingyun.feng@ucr.edu

[**] We thank the support of this work by the NSF (X.B. DMR-0846958), the DOE (P.F. DE-SC0002235), and NIH-RISE (R.N. GM071638). X.B. is a Henry Dreyfus Teacher Scholar.

Supporting information for this article is available on the WWW under http://dx.doi.org/10.1002/anie.201001675.

Another consideration involves the local charge distribution and overall charge of the target framework. Since $[B(im)_4]^-$ readily forms neutral zeolite-type frameworks with monovalent Li and Cu ions (e.g., $LiB(im)_4$), the combination of higher charged metal ions such as Zn^{2+} with $[B(im)_4]^-$ would likely result in positively charged structural subunits (chains, layers, or even 3D frameworks). The introduction of di- or polycarboxylates with a higher charge density (−2, −3, etc. per ligand) than imidazolates (−1 per ligand) can provide charge compensation for the positively charged $M^{2+}/[B(im)_4]^-$ subunits, leading to the formation of neutral MC-BIFs.

Herein, we report a family of MC-BIFs that integrate both carboxylate and imidazolate building blocks. MC-BIF-1S through to MC-BIF-5H all possess 3D framework structures, whereas MC-BIF-6S has a 3-connected ladderlike structure. The use of both hydro- and solvothermal conditions in this work is noteworthy. MOFs are generally prepared under solvothermal conditions and many have limited hydrothermal stability. Since the hydrothermal stability is key to some applications of MOFs, it has been desirable to synthesize MOFs under hydrothermal conditions. Herein, MC-BIF-1S, MC-BIF-4S, and MC-BIF-6S were solvothermally synthesized whereas MC-BIF-2H, MC-BIF-3H, and MC-BIF-5H were prepared by hydrothermal synthesis.

Chiral MC-BIF-1S is the first example that integrates the bonding features in all three families of materials (i.e., MCFs, ZIFs, and BIFs). Despite such a complex composition, its topology is very simple. One fundamental feature of MC-BIF-1S is the pentagonal layer parallel to the *ab* plane (Figure 1a). Within the layer, only pentagonal rings consisting of two B and three Zn sites are observed, and each Zn^{2+} site is bonded to two $[B(im)_4]^-$ complexes and one free im ligands ("free" meaning that this imidazolate ligand is not a part of the covalent $[B(im)_4]^-$ complex). Each boron site is 4-connected to four separate Zn sites.

The aforementioned pentagonal layer was previously observed in ZBIF-1 with the formula of $[Zn_2(im)Cl_2\{B(im)_4\}]$.[10] However, because of the rich chloride environment in the deep eutectic solvent (choline chloride/*N*,*N*′-dimethylurea) used for the synthesis of ZBIF-1, the fourth Zn^{2+} coordination site in ZBIF-1 is terminated by Cl^-, leading to an overall lamella structure. By replacing terminal Cl^- anions with cross-linking ligands, it should be possible to convert 2D ZBIF-1 into a 3D framework. In this work, we identified a unique combination of cross-linker and solvent that allowed us to achieve this goal. By eliminating the Cl^- source and employing the solvent 1,3-dimethylpropyleneurea, the B/im/Zn pentagonal layers were pillared through Zn–bdc–Zn linkages (Table 1; bdc = 1,4-benzenedicarboxy-

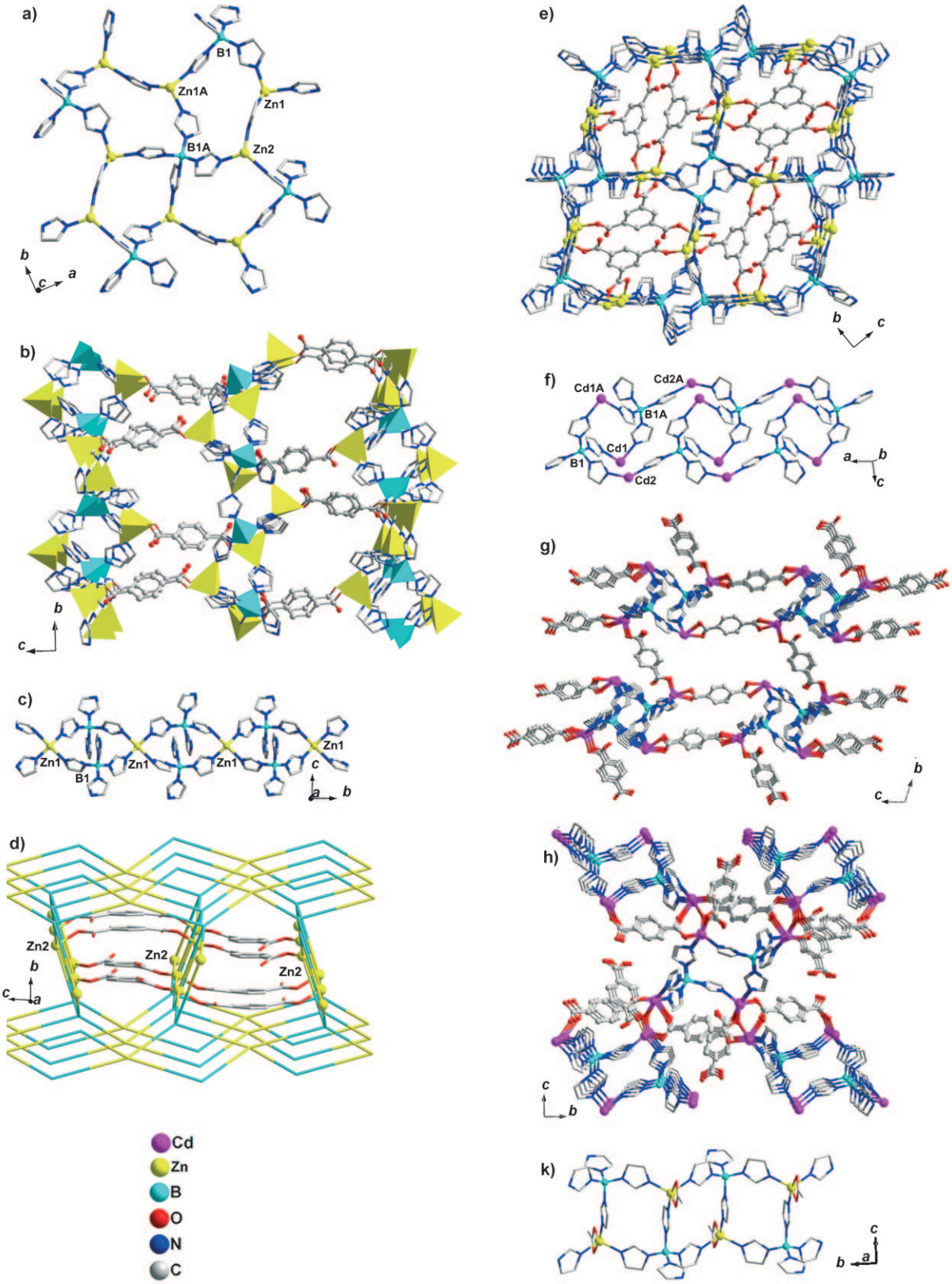

Figure 1. a,b) Views of 2D B/im/Zn layer and 3D structure of MC-BIF-1S, respectively. ZnN_3O tetrahedron: yellow; BN_4 tetrahedron: blue. c,d) Views of 1D B/im/Zn chain and 3D structure of MC-BIF-2H, respectively. All 2-connected im ligands were simplified as lines. e) View of 3D structure of MC-BIF-3H. f,g) Views of 1D B/im/Cd tube and 3D structure of MC-BIF-4S, respectively. The neutral Him and *p*-murea ligands are omitted for clarity. h) View of 3D structure of MC-BIF-5H. k) 1D double-chain structure in MC-BIF-6S.

Table 1: Summary of crystal data and refinement results.

Compound	Formula	Space group	*a* [Å]	*b* [Å]	*c* [Å]	α [°]	β [°]	γ [°]	*R*(F) [%]
MC-BIF-1S	$[Zn_2(im)(bdc)][B(im)_4]\cdot p$-murea	$P4_32_12$	13.0584(18)	13.0584(18)	53.7310(11)	90	90	90	8.00
MC-BIF-2H	$[Zn_3(bdc)_2(H_2O)][B(im)_4]_2\cdot 2H_2O$	$C2/c$	13.1669(14)	21.2270(2)	18.2540(2)	90	106.787(7)	90	5.17
MC-BIF-3H	$[Zn_2(btc)][B(im)_4]\cdot 3H_2O$	$P2_1/c$	11.8587(15)	13.7752(16)	16.7460(2)	90	96.469(7)	90	5.42
MC-BIF-4S	$[Cd(Him)(p\text{-murea})][Cd(bdc)_{1.5}]$-$[B(im)_4]\cdot p$-murea	$P\bar{1}$	9.3195(2)	14.2603(2)	18.4982(4)	105.307(1)	99.077(1)	95.406(1)	3.67
MC-BIF-5H	$[Cd_2(bdc)(Hbdc)][B(im)_4]\cdot 0.5H_2O$	$P2_1/c$	8.8738(5)	18.3991(9)	20.1384(10)	90	98.843(1)	90	3.22
MC-BIF-6S	$[Zn(OAc)][B(im)_4]$	*Pnma*	13.5313(7)	9.9802(5)	12.7491(7)	90	90	90	4.15

late) into a 3D framework, called MC-BIF-1S herein (Figure 1b).

MC-BIF-2H illustrates the effect of solvents on the self-assembly process in the Zn–$[B(im)_4]$–bdc system. One notable difference, relative to MC-BIF-1S, is that the free imidazolate ligand (in the form of Zn–im–Zn) is no longer present, suggesting the possible lower hydrothermal stability the M^{II}–im–M^{II} linkage relative to the M^{II}–im–B^{III} linkage. Another difference is the coordination of water to one of two unique Zn sites, an obvious effect of the hydrothermal synthesis (Figure S2 in the Supporting Information). Each Zn1 ion is coordinated to four im ligands and one water molecule to form a distorted trigonal bipyramidal configuration, whereas each Zn2 ion is tetrahedrally bonded to two im ligands and two O donors from two bdc ligands. As shown in Figure 1c, two Zn1 ions are bridged by two $[B(im)_4]^-$ groups to form a four-ring, which further extends into a 1D B/im/Zn chain by sharing zinc corners. Next, each 1D Zn/$[B(im)_4]^-$ chain is connected to four adjacent chains through Zn2 ions to yield a 3D Zn/$[B(im)_4]^-$ framework with 1D channels in which the bdc ligands are located (Figure 1d, Figure S3 in the Supporting Information). Such bdc ligands bridge Zn2 ions by completing their two remaining coordination sites. It is worth noting that even without considering cross-linking by dicarboxylates, the connectivity between Zn^{2+} and $[B(im)_4]^-$ alone is 3D.

MC-BIF-1S and MC-BIF-2H demonstrate the feasibility to synthesize MC-BIFs under hydrothermal or solvothermal conditions. We then further examined the versatility of our synthetic method by expanding from the dicarboxylate system to the tricarboxylate system, which led to the hydrothermal synthesis of MC-BIF-3H. Again, as in MC-BIF-2H, there is no M^{II}–im–M^{II} linkage in MC-BIF-3H, which is consistent with our earlier observation of possibly higher hydrothermal stability of M^{II}–im–B than of M^{II}–im–M^{II}.

MC-BIF-3H can be considered as built from the 2D B/im/Zn layer pillared by the carboxylate ligands. There are two unique tetrahedral zinc sites (Figure S4 in the Supporting Information), which are bonded to two N and two O atoms from two im and two btc ligands (btc = 1,3,5-benzenetricarboxylate). MC-BIF-3H consists of two types of macrocyclic $B_4Zn_4(im)_8$ eight-rings (Figure S5 in the Supporting Information): one is a square-type eight-ring and the other is an elongated narrow-type eight-ring. Every square-type eight-ring shares its four edges with four narrow-type eight-rings, and vice versa, resulting in 2D Zn/$[B(im)_4]$ layers that are further linked by btc ligands to yield a 3D structure (Figure 1e).

When using mixed cross-linking ligands, their ratio and the role of each ligand in determining the dimensionality of the overall framework are of significance in the control of framework composition and topology. As discussed above, in MC-BIF-1S and MC-BIF-3H, the M^{2+}/im/B connectivity is 2D and the connectivity in the third dimension is established by bridging carboxylate ligands. In comparison, MC-BIF-2H possesses the 3D M^{2+}/im/B connectivity with the charge-balancing carboxylate ligand completing the remaining Zn coordination sites.

Herein we demonstrate that the competing role of different ligands (i.e., carboxylates and imidazolates) can be tuned. Specifically, it is possible to broaden the dimensionality of M^{2+}/im/B connectivity to include 1D, and in the meantime to increase the dimensionality of the M^{2+}/carboxylate connectivity. Such a change in the dimensionality of the metal–ligand substructure connectivity is generally accompanied by a change in the carboxylate/$[B(im)_4]^-$ ratio within the framework. In this case, the use of a metal ion (Cd^{2+} in this work) with the ionic radius larger than Zn^{2+} offers an insight into the correlation between the overall structure and its atomic building blocks.

The use of Cd^{2+} to vary the carboxylate/$[B(im)_4]^-$ ratio and to tune the dimensionality of M^{2+}/carboxylate and M^{2+}/B/im substructures can involve the following two factors: 1) the carboxylate can be the chelating ligand whereas $[B(im)_4]^-$ can not; 2) because of the larger ionic radius, Cd^{2+} has a greater tendency to form a chelate than Zn^{2+}. These two factors are likely the reason for the increased carboxylate/$[B(im)_4]^-$ ratio and a reduction in the M^{2+}/im/B connectivity to 1D in two new MC-BIFs made with Cd^{2+} (in all zinc compounds herein, the carboxylate/$[B(im)_4]^-$ ratio is 1).

MC-BIF-4S and MC-BIF-5H, in which the carboxylate/$[B(im)_4]^-$ ratio is 1.5 and 2, respectively, are constructed from 1D Cd^{2+}/$[B(im)_4]^-$ tubes linked by bdc ligands into 3D structures. In MC-BIF-4S, there are two unique Cd sites (Figure S6 in the Supporting Information). The six-coordinate Cd1 only serves as a 3-connected node to two B atoms and one Cd atom through two im ligands (nonchelating) and one bdc ligand (chelating), respectively. There are two terminal ligands, one Him and one *p*-murea (*p*-murea = 1,3-dimethylpropyleneurea). The five-coordinate Cd2 acts as a 4-connected node cross-linked to two B atoms and two Cd atoms through two im ligands and two bdc ligands, respectively.

Thus, the 3D structure of MC-BIF-4S can be described as follows. First, as shown in Figure 1 f, every two Cd1 ions and two $[B(im)_4]^-$ groups are alternately joined together through Cd–im–B linkages to form a $B_2Cd_2(im)_8$ four-ring. Then, the adjacent four-rings are further bridged by two Cd2 ions along the *a* axis to generate an infinite B/im/Cd tube. Finally, these tubes are cross-linked along the *b* and *c* directions to generate a 3D framework (Figure 1 g). This structural feature of MC-BIF-4S is similar to that of a recently reported zincophosphate constructed from 1D zinc phosphate four-ring columns interlinked by organic ligands.[11]

By switching from a solvothermal to a hydrothermal method in the Cd system, a new 3D structure MC-BIF-5H was obtained. The structure of 1D B/im/Cd tube in MC-BIF-5H is similar to that in MC-BIF-4S (Figure S7 in the Supporting Information). These B/im/Cd tubes are further joined together through COO^- groups to form a 3D framework (Figure 1 h). The effect of hydrothermal synthesis again reveals itself through the inclusion of water molecules in MC-BIF-5H.

From MC-BIF-1S through to MC-BIF-5H, bridging di- or tricarboxylates were used. With a monocarboxylate ligand (acetate in this case), it was possible to obtain crystals that contain isolated low-dimensional M/carboxylate/$B(im)_4$ structures that are potential structural building blocks in higher dimensional structures. One such structure is MC-BIF-6S with a 1D double-chain structure. MC-BIF-6S is made up of $\{[Zn(OAc)_2]_2[B(im)_4]_2\}$ four-rings (Figure 1 k). Similar four-ring structures are also observed in MC-BIF-2H, MC-BIF-4S, and MC-BIF-5H. However, unlike the four-rings in MC-BIF-2H which are corner-sharing or the four-rings in MC-BIF-4S and -5H which are isolated, the four-rings in MC-BIF-6S share edges to form a ladder-type structure.

The total potential solvent-accessible volumes of solvothermal products MC-BIF-1S and MC-BIF-4S, calculated with PLATON,[12] are 52.2% and 47.8%, respectively. In comparison, the potential solvent-accessible volumes of hydrothermal products (MC-BIF-2H: 13.7%; MC-BIF-3H: 18.7%; MC-BIF-5H: 11.3%) are much smaller, which may be related to the size of the solvent molecule. However, as shown below, the actual measured porosity does not correlate with the calculated trend, which is likely to be caused by the pore geometry and the degree of solvent removal in each case.

Gas-adsorption measurements (H_2, CO_2, and N_2) were performed on a Micromeritics ASAP 2010 surface-area and pore-size analyzer, which confirmed the permanent microporosity of MC-BIF-2H, MC-BIF-3H, and MC-BIF-5H (Figure 2). These samples were degassed at 150 °C for 24 h under vacuum prior to the measurement. Figure 2 shows the dependence of gas-sorption properties on the crystal structure. The maximum CO_2 adsorptions of MC-BIF-2H, MC-BIF-3H, and MC-BIF-5H at 273 K and 1 atm are 54.3, 36.4, and 5.3 $cm^3 g^{-1}$, respectively. The CO_2 uptake capacity, especially the volumetric storage capacity, of MC-BIF-2H (81 $L L^{-1}$) at 1 atm and 273 K is very high, particularly considering its relatively low percentage of solvent-accessible volume (only 13.7%). Such a high CO_2 storage capacity was further verified by multiple samples made from repeated syntheses and three independent adsorption measurements.

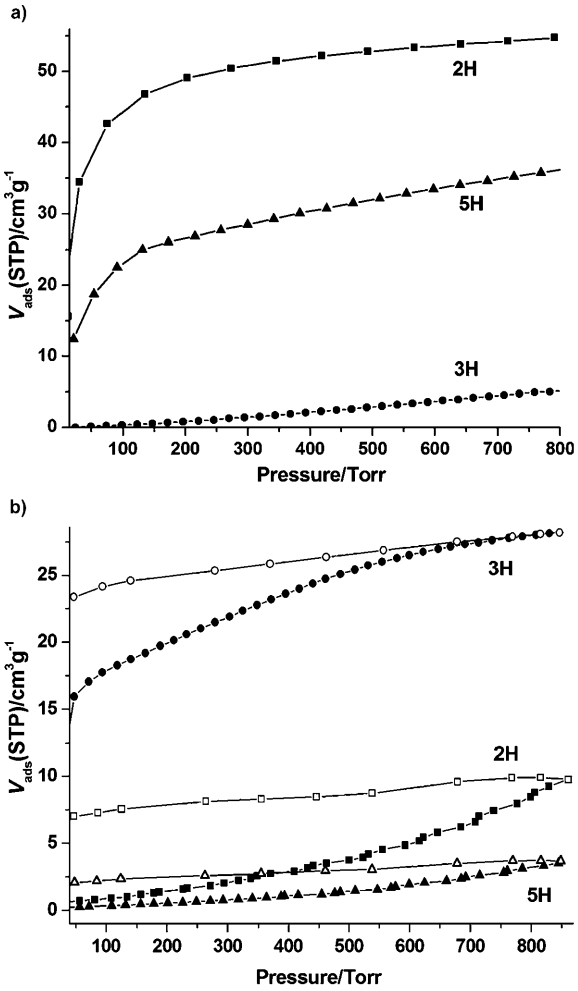

Figure 2. a) CO_2 adsorption isotherms of MC-BIF-2H (■), MC-BIF-3H (●), and MC-BIF-5H (▲). b) H_2, adsorption (■, ●, ▲) and desorption (□, ○, △) isotherms of MC-BIF-2H, MC-BIF-3H, and MC-BIF-5H.

In comparison, the volumetric CO_2 storage capacity for ZIF-69 is about 83 $L L^{-1}$ under the same condition.[13]

To gain insight into the high CO_2 adsorption capacity, thermogravimetric data of MC-BIF-2H were analyzed, which gives the first weight loss (4.66%) in the range 120–220 °C and no further weight loss up to 300 °C (Figure S11 in the Supporting Information), which is in good agreement with the removal of both extraframework and terminal water molecules (4.75%). We further examined the water loss and the associated structural change by temperature-dependent single-crystal X-ray diffraction. The refinement results show that after heating at 220 °C for 2 h, the single crystal remains stable and that both extraframework and terminal water molecules can be removed (see the Supporting Information), leading to open metal sites on Zn1 (Figure S13).

The open Zn^{2+} site in MC-BIF-2H is different from other M^{2+} sites in the MC-BIF series, because it is bonded to $[B(im)_4]^-$ complexes whereas in other structures each M^{2+} site is bonded to at least one carboxylate end. Compared to ZIFs, this open zinc site is also special because the negative charge of four adjacent imidazolate ligands is drawn more toward B^{3+} in MC-BIF-2H. It is thus expected that the open Zn^{2+} site

in MC-BIF-2H receives less negative charge from adjacent ligands and has a correspondingly higher level of the local positive charge, which likely makes it more polarizing. The net result is likely an increased interaction with CO_2, leading to an enhanced CO_2 adsorption capacity.[14] Additionally, because of the small kinetic diameter of CO_2, the large pore window or large cage cavity is not essential for efficient adsorption. In MC-BIF-2H, the pore space formed by the 3D metal–boron–imidazolate framework is further partitioned by dicarboxylates into smaller pore regions, which may also help enhance the CO_2 storage. This result is consistent with the previous observations that interpenetration and extraframework species can enhance gas sorption properties, even though the pore space may be reduced.[15]

The H_2 adsorption isotherms of MC-BIF-2H, MC-BIF-3H, and MC-BIF-5H at 77 K and 1 atm give uptakes of 9.9, 28.2, and 3.7 $cm^3 g^{-1}$, respectively. Possibly because of the small pore aperture in these MC-BIFs, the H_2 adsorption/desorption isotherms of these samples are distinctly hysteretic (Figure 2). Although these compounds showed CO_2 and H_2 adsorption, no significant N_2 adsorption was observed, which is likely a result of the limitation of the aperture size.

In summary, we have prepared a new family of porous materials (MC-BIFs) by integrating metal carboxylates and boron imidazolates. The rich synthetic and structural chemistry of the MC-BIF system has been demonstrated through both hydro- and solvothermal synthesis with different metal ions (Zn^{2+} or Cd^{2+}) and different carboxylates (bdc and btc), in conjunction with $[B(im)_4]^-$ complexes and "free" imidazolate ligand. The dimensionality of M/carboxylate and M/$[B(im)_4]$ substructures can also be tuned to create new framework materials with tunable gas-sorption properties. Among these new materials, the hydrothermally synthesized MC-BIF-2H exhibits a very high volumetric CO_2 storage capacity of 81 $L L^{-1}$, which is comparable to 83 $L L^{-1}$ previously reported for a highly porous ZIF-69.

Received: March 20, 2010
Revised: May 5, 2010
Published online: June 25, 2010

Keywords: boron · carboxylate ligands · metal–organic frameworks · microporous materials · nitrogen heterocycles

[1] J. Long, O. M. Yaghi, *Chem. Soc. Rev.* **2009**, *38*, 1213 – 1504.
[2] G. Férey, *Chem. Soc. Rev.* **2008**, *37*, 191.
[3] a) S. S. Y. Chui, S. M.-F. Lo, J. P. H. Charmant, A. G. Orpen, L. D. Williams, *Science* **1999**, *283*, 1148; b) H. Li, M. Eddaoudi, M. O'Keeffe, O. M. Yaghi, *Nature* **1999**, *402*, 276; c) G. Férey, C. Mellot-Draznieks, C. Serre, F. Millange, J. Dutour, S. Surblé, I. Margiolaki, *Science* **2005**, *309*, 2040; d) S. Yang, X. Lin, A. J. Blake, G. Walker, P. Hubberstey, N. R. Champness, M. Schröder, *Nat. Chem.* **2009**, *1*, 487; e) X. Zhao, B. Xiao, A. J. Fletcher, K. M. Thomas, D. Bradshaw, M. J. Rosseinsky, *Science* **2004**, *306*, 1012.
[4] a) B. Xiao, P. J. Byrne, P. S. Wheatley, D. S. Wragg, X. Zhao, A. J. Fletcher, K. M. Thomas, L. Peters, J. S. O. Evans, J. E. Warren, W. Zhou, R. E. Morris, *Nat. Chem.* **2009**, *1*, 289; b) L. Ma, A. Jin, Z. Xie, W. Lin, *Angew. Chem.* **2009**, *121*, 10089; *Angew. Chem. Int. Ed.* **2009**, *48*, 9905; c) K. Koh, A. G. Wong-Foy, A. J. Matzger, *J. Am. Chem. Soc.* **2009**, *131*, 4184; d) T. Tsuruoka, S. Furukawa, Y. Takashima, K. Yoshida, S. Isoda, S. Kitagawa, *Angew. Chem.* **2009**, *121*, 4833; *Angew. Chem. Int. Ed.* **2009**, *48*, 4739.
[5] a) B. Chen, L. Wang, Y. Xiao, F. R. Fronczek, M. Xue, Y. Cui, G. Qian, *Angew. Chem.* **2009**, *121*, 508; *Angew. Chem. Int. Ed.* **2009**, *48*, 500; b) D. Zhao, D. Yuan, D. Sun, H. C. Zhou, *J. Am. Chem. Soc.* **2009**, *131*, 9186; d) J. Zhang, L. Wojtas, R. W. Larsen, M. Eddaoudi, M. J. Zaworotko, *J. Am. Chem. Soc.* **2009**, *131*, 17040; c) H. J. Park, M. P. Suh, *Chem. Commun.* **2010**, *46*, 610.
[6] a) A. Demessence, D. M. D'Alessandro, M. L. Foo, J. R. Long, *J. Am. Chem. Soc.* **2009**, *131*, 8784; b) K. Sumida, M. R. Hill, S. Horike, A. Dailly, J. R. Long, *J. Am. Chem. Soc.* **2009**, *131*, 15120; c) Y. B. Zhang, W. X. Zhang, F. Y. Feng, J. P. Zhang, X. M. Chen, *Angew. Chem.* **2009**, *121*, 5391; *Angew. Chem. Int. Ed.* **2009**, *48*, 5287; d) A. Sonnauer, F. Hoffmann, M. Fröba, L. Kienle, V. Duppel, M. Thommes, C. Serre, G. Férey, N. Stock, *Angew. Chem.* **2009**, *121*, 3849; *Angew. Chem. Int. Ed.* **2009**, *48*, 3791; e) T. Ahnfeldt, N. Guillou, D. Gunzelmann, I. Margiolaki, T. Loiseau, G. Férey, J. Senker, N. Stock, *Angew. Chem.* **2009**, *121*, 5265; *Angew. Chem. Int. Ed.* **2009**, *48*, 5163; f) K. L. Mulfort, O. K. Farha, C. D. Malliakas, M. G. Kanatzidis, J. T. Hupp, *Chem. Eur. J.* **2010**, *16*, 276.
[7] a) M. H. Alkordi, J. A. Brant, L. Wojtas, V. C. Kravtsov, A. J. Cairns, M. Eddaoud, *J. Am. Chem. Soc.* **2009**, *131*, 17753; b) K. Li, D. H. Olson, J. Seidel, T. J. Emge, H. Gong, H. Zeng, J. Li, *J. Am. Chem. Soc.* **2009**, *131*, 10368; c) H. B. Wu, Q. M. Wang, *Angew. Chem.* **2009**, *121*, 7479; *Angew. Chem. Int. Ed.* **2009**, *48*, 7343; d) Y. Qiu, H. Deng, J. Mou, S. Yang, M. Zeller, S. R. Batten, H. Wue, J. Lie, *Chem. Commun.* **2009**, 5415; e) J. An, S. J. Geib, N. L. Rosi, *J. Am. Chem. Soc.* **2010**, *132*, 38; f) Y. Q. Tian, S. Y. Yao, D. Gu, K. H. Cui, D. W. Guo, G. Zhang, Z. X. Chen, D. Y. Zhao, *Chem. Eur. J.* **2010**, *16*, 1137.
[8] a) Z. Lu, C. B. Knobler, H. Furukawa, B. Wang, G. Liu, O. M. Yaghi, *J. Am. Chem. Soc.* **2009**, *131*, 12532; b) A. Phan, C. J. Doonan, F. J. Uriberomo, C. B. Knobler, M. O'Keefee, O. M. Yaghi, *Acc. Chem. Res.* **2010**, *43*, 58.
[9] a) J. Zhang, T. Wu, C. Zhou, S. Chen, P. Feng, X. Bu, *Angew. Chem.* **2009**, *121*, 2580; *Angew. Chem. Int. Ed.* **2009**, *48*, 2542; b) T. Wu, J. Zhang, C. Zhou, L. Wang, X. Bu, P. Feng, *J. Am. Chem. Soc.* **2009**, *131*, 6111.
[10] S. Chen, J. Zhang, T. Wu, P. Feng, X. Bu, *Dalton Trans.* **2010**, *39*, 697.
[11] S. H. Huang, C. H. Lin, W. C. Wu, S. L. Wang, *Angew. Chem.* **2009**, *121*, 6240; *Angew. Chem. Int. Ed.* **2009**, *48*, 6124.
[12] A. L. Spek, *Platon*, Utrecht University, The Netherlands, **2003**.
[13] R. Banerjee, A. Phan, B. Wang, C. Knobler, H. Furukawa, M. O'Keeffe, O. M. Yaghi, *Science* **2008**, *319*, 939.
[14] a) M. Dincă, J. R. Long, *Angew. Chem.* **2008**, *120*, 6870; *Angew. Chem. Int. Ed.* **2008**, *47*, 6766; b) H. Wu, W. Zhou, T. Yildirim, *J. Am. Chem. Soc.* **2009**, *131*, 4995.
[15] a) L. Ma, W. Lin, *Angew. Chem.* **2009**, *121*, 3691; *Angew. Chem. Int. Ed.* **2009**, *48*, 3637; b) S. Chen, J. Zhang, T. Wu, P. Feng, X. Bu, *J. Am. Chem. Soc.* **2009**, *131*, 16027.

